8-16-2013

Cyclic Durability of a Solid Oxide Fe-Air Redox Battery Operated at 650°C

Xuan Zhao

Yunhui Gong

Xue Li

Nansheng Xu

Kevin Huang
University of South Carolina - Columbia, huang46@cec.sc.edu

Publication Info

Published in *Journal of The Electrochemical Society*, Volume 160, Issue 10, 2013, pages A1716-A1719.

Publisher's Version: http://dx.doi.org/10.1149/2.048310jes
Zhao, X., Gong, Y., Li, X., Xu, N., & Huang, K. (2013). Cyclic Durability of a Solid Oxide Fe-Air Redox Battery Operated at 650°C. Journal of The Electrochemical Society, 160 (10), A1716 - A1719. http://dx.doi.org/10.1149/2.048310jes

Journal of The Electrochemical Society, **160** (10) A1716-A1719 (2013)
0013-4651/2013/160(10)/A1716/4/$31.00 © The Electrochemical Society

Cyclic Durability of a Solid Oxide Fe-Air Redox Battery Operated at 650°C

Xuan Zhao,* Yunhui Gong, Xue Li, Nansheng Xu, and Kevin Huang,z**

Department of Mechanical Engineering, University of South Carolina, South Carolina 29201, USA

The recently developed rechargeable solid oxide metal-air redox battery has shown a great potential for applications in mid- to large-scale stationary energy storage. Cyclic durability is one of the most important requirements for stationary energy storage. In this study, we report the cyclic durability of a solid oxide Fe-air redox battery operated at 650°C. The battery was continuously cycled 100 times under a current density of 50 mA/cm^2 with rather flat performance, producing an average specific energy of 760 Wh/kg-Fe at a round-trip efficiency of 55.5%. The post-test examination indicated that the performance losses could arise from the fuel-electrode of the battery.
 [DOI: 10.1149/2.048310jes]

Manuscript submitted July 8, 2013; revised manuscript received April 1, 2013. Published August 16, 2013.

High energy-capacity metal-air batteries have drawn considerable interest as a potential electrochemical device for mid- to large-scale stationary energy storage.[1–10] Among various metal-air chemistries, investigations on high energy-capacity lithium-air batteries are the primary focus. However, issues like irreversibility of the electrode reactions, clogging of the air-pathway, and decomposition or evaporation of the organic electrolytes make rechargeable lithium-air batteries a formidable challenge.[1,2,7,8] Therefore, new metal-air chemistries that can lead to advanced metal-air batteries with good reversibility and cyclic life are greatly needed.

Recently, our group demonstrated a new class of solid oxide metal-air redox batteries (SOMARBs) that use chemically stable solid oxide-ion electrolytes and involve only gaseous O_2 at the air-electrode during the charge/discharge reactions.[11–16] These unique features can easily overcome the critical problems facing the lithium-air battery, e.g. electrolyte/electrode interactions and formation of air-pathway clogging phases. As previously described,[11–16] a typical SOMARB consists of two key components: a reversible solid oxide fuel cell (RSOFC) and a metal/metal-oxide redox couple. The former functions as the electrical functioning unit (EFU) to realize the charge/discharge cycle, while the latter serves as the chemical energy storage medium (ESM). As a means of facilitating the kinetics of redox reaction, a mixture of H_2-H_2O is also employed as an oxygen shuttle moving between EFU and ESM. In specific, during the discharge cycles, the RSOFC works as a fuel cell, in which H_2 produced from the steam-metal reaction in the ESM is electrochemically oxidized by O^{2-} to produce water that migrates back to the ESM to sustain the steam-metal reaction. During the charge cycles, the RSOFC works as an electrolyzer and all the reactions occurring in RSOFC and ESM during the discharge cycles reverse their directions.[11–16]

With the earth-abundant and environmentally benign Fe as the redox active metal, we first demonstrated the SOMARB with the Fe/FeO redox couple in a tubular cell configuration,[12] and later studied their energy storage characteristics under various testing conditions with a planar cell configuration.[13] Recently, we also reported promising results of a 550°C-SOMARB using the high-capacity Fe-Fe_3O_4 redox couple as the ESM.[11] Similar works have also been reported by other research groups.[17–20] However, among all the published results, cyclic durability of such a high-temperature redox battery, a very important requirement for stationary applications, has not been reported.

In this study, we aim to fill this gap by testing the cyclic durability of a SOMARB based on Fe-FeO redox couple. We chose 650°C as the temperature of evaluation because the development of RSOFCs is well established within this temperature range. In addition, the thermodynamically stable redox-couple at 650°C is Fe-FeO, where abundant point-defects are available in $FeO_{1-\delta}$ to ensure good redox kinetics.[12,13] The long-term stability of SOMARB with the Fe-Fe_3O_4 redox couple operated at 550°C is currently being tested in our lab, the results of which will be reported in the near future.

Experimental

Battery assembly.— The battery for the endurance test was assembled in a planar button cell configuration as described previously.[11] The Fe-FeO redox couple in the battery's ESM was derived from a precursor Fe_2O_3-ZrO_2 synthesized by a chemical co-precipitation method.[11–13] The RSOFC consisted of a tape-casted $La_{0.8}Sr_{0.2}Ga_{0.83}Mg_{0.17}O_{3-\delta}$ (LSGM) electrolyte membrane,[21,22] a porous LSGM-based air-electrode infiltrated with $Sm_{0.5}Sr_{0.5}CoO_{3-\delta}$ (SSC)-$Sm_{0.2}Ce_{0.8}O_{1.9}$ (SDC)[23] and a Ni-CeO_2 based cermet fuel-electrode, all homemade in our lab. The active cell area was 1.30 cm^2. Table I summarizes the compositions and thickness of the functional layers employed in the RSOFC. The Fe-FeO based ESM was situated next to but not in direct contact with the fuel-electrode. A homemade glass was used to seal the battery. Readers can refer to our previous publications for more experimental details.[11–13]

Battery characterization.— At the beginning of the test, the battery cell was heated up with Fe_2O_3-ZrO_2 granules (ESM precursor) being exposed to a mixture of 5%H_2 and N_2. Once reached the melting temperature of the sealing glass at 650°C, the 5%H_2-N_2 gas was switched to a pure H_2 humidified with 3% H_2O for final reduction of Fe_2O_3 into Fe. When the reduction process was completed, both the H_2 inlet and outlet were closed off and the fuel-electrode became a closed chamber. To create the Fe-FeO redox couple, a small discharge current (10 mA/cm^2) from the RSOFC was applied. To ensure the attainment of Fe-FeO equilibrium without over-consuming the active Fe, EMF of the RSOFC was closely monitored during the electrochemical oxidation by intermittently switching between the discharging and OCV states. As soon as the EMF reached 1.03 volts, the theoretical Nernst potential for the Fe-FeO equilibrium at 650°C, the electrochemical oxidation was stopped, and the system was ready for the charge-discharge cycles. A Solartron 1260/1287 Electrochemical System was employed to characterize the electrical performance of

Table I. Materials employed in RSOFC of the solid oxide Fe-air redox battery operated at 650°C.

Component	Composition	Thickness (μm)
Fuel electrode	LDC-Ni/GDC-Ni	30
Electrolyte	LSGM	180
Air electrode	Porous LSGM- SSC/SDC	50
Current collector	Silver mesh & paste for air-electrode/platinum mesh for fuel-electrode	10

LDC = $La_{0.4}Ce_{0.6}O_{2-\delta}$; GDC = $Gd_{0.2}Ce_{0.8}O_{2-\delta}$

*Electrochemical Society Student Member.
**Electrochemical Society Active Member.
zE-mail: kevin.huang@sc.edu

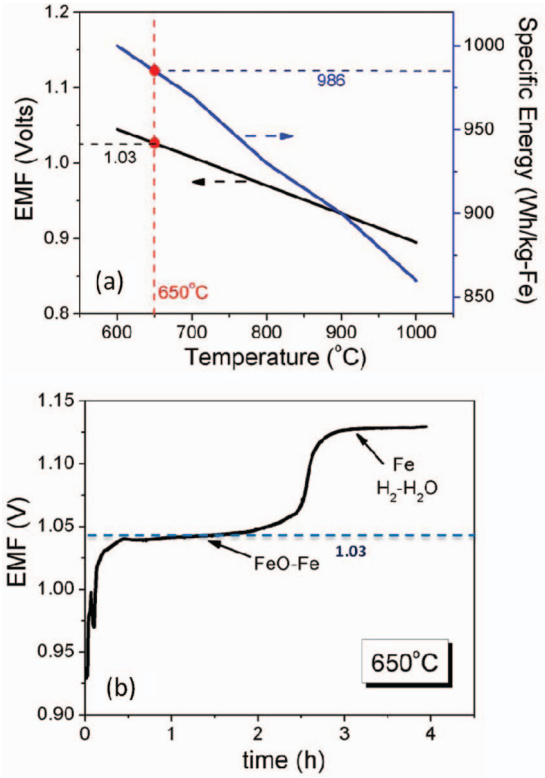

Figure 1. (a) Plots of theoretical Nernst potential (EMF) and specific energy over temperatures of the solid oxide Fe-air redox battery using Fe-FeO redox couple as the ESM; (b) experimentally recorded EMF curve during the reduction of Fe_2O_3 by H_2-3%H_2O at 650°C.

the battery under various operating conditions with software modules such as OCV-t, impedance spectroscopy, and galvanic cycles.

The microstructures and compositions of RSOFC and ESM, either in pre-tested or post-tested state, were examined with a field-emission scanning electron microscopy (FESEM, Zeiss Ultra) equipped with EDX.

Results and Discussion

Confirmation of the Fe-FeO equilibrium.— One pronounced feature of the new solid oxide Fe-air redox battery is that the Fe-based ESM is spatially decoupled from the RSOFC, thus yielding a state-of-charge independent EMF.[11,13–15] Monitoring of EMF can help verify the phase equilibrium in the Fe-FeO_x redox couples. Thermodynamic analysis suggests that the stable redox couple is Fe-FeO at t > 600°C,[11,15] the Maximum Theoretical Specific Energy (MTSE) and EMF of which are given in Fig. 1a as a function of temperatures. At t = 650°C, the MTSE and EMF are 986 Wh/kg-Fe and 1.03 V, respectively. The experimental EMF recorded during H_2 reduction in Fig. 1b confirms the EMF predicted by Fig. 1a; the EMF plateau observed at 1.03 V corresponds excellently to the thermodynamic value of the Fe-FeO equilibrium. The plateau with higher EMF at 1.125 V represents metallic Fe coexisting with H_2-3%H_2O in the system.

Cyclic durability.— The cyclic durability of the battery was examined at 650°C by continuously subjecting the battery to discharge and charge current density of J = 50 mA/cm^2 for 100 times. The duration of each single discharge or charge cycle was set to 10 min. It is evident from Fig. 2a that the cycling performance is rather stable; only a slight degradation is seen for the first 20 cycles. More specifically, the degradation during the first 5 cycles is observed for both the discharge and charge cycles, after which the degradation is only found for the charge cycle until 20 cycles. After 20 cycles, no obvious degradation can be discerned for all the cycles. The average discharge specific energy over 100 cycles is 760 Wh/kg-Fe as shown in Fig. 2b, which is about 77.1% of MTSE. When compared with the average charge specific energy (=1,370 Wh/kg-Fe), the battery cycled at a round-trip efficiency of 55.5%. This performance, despite its insufficiency to commercial applicability, is better than the same type of Fe-air cell using an YSZ electrolyte operated at 1000°C, in which the average round-trip efficiency over 10 continuous cycles was only 12%.[19]

It should be noted that the specific energy shown in Fig. 2b is normalized to the mass of the Fe consumed by the oxygen flux

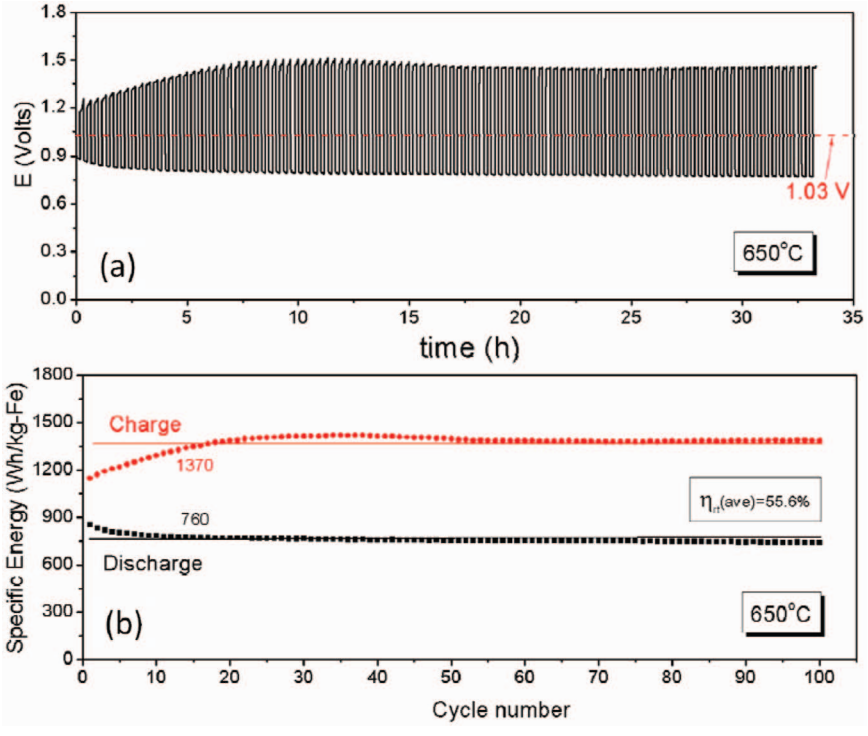

Figure 2. (a) Discharge and charge characteristics of the battery at 650°C and J = 50 mA/cm^2; (b) Plot of specific energy as a function of the number of discharge and charge cycles.

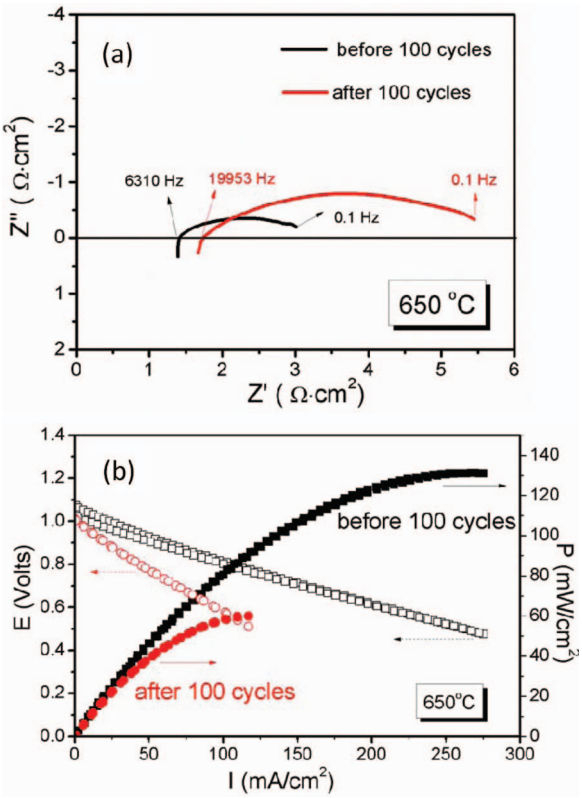

Figure 3. Electrical performance of RSOFC measured under the open circuit and 650°C. (a) Impedance spectra; (b) P-I and V-I curves before and after 100 galvanic cycles.

(corresponding to the current of RSOFC) in order to support the redox reaction. Such normalization allows for comparison with theoretical values such as those shown in Fig. 1 and other published results. The lowered discharge specific energy and round-trip efficiency signal that some of energy has been lost to electrochemical polarizations of the RSOFC and kinetic resistances of the redox reactions.

Electrochemical impedance analysis.— To investigate the root cause of the degradation, impedance spectra and V-I curves of the battery before and after the test were measured, the results of which are shown in Fig. 3. The impedance spectra of Fig. 3a clearly show increases in area-specific resistances (ASRs) of ohmic and polarization portions after 100 discharge/charge cycles. The total ASR of the battery was increased from 3.01 to 5.48 $\Omega \cdot cm^2$. The increase in polarization ASR is much severer than that of ohmic ASR, 2.14 Ωcm^2 vs 0.33 Ωcm^2. The reduction in power density of RSOFC shown in Fig. 3b corresponds to the increases in ASR obtained from electrochemical impedance study, decreasing from the original 131 to 60 mW/cm^2 after 100 cycles. The after-100-cycle performance degradation shown in Fig. 3 seems to suggest that the initial degradation as shown in Fig. 2b could be related to the RSOFC employed.

Microstructural examination.— To further investigate why the battery's initial performance has degraded, microscopic examination on the RSOFC was carried out. Fig. 4a shows the RSOFC consisting of all the three functional layers: air-electrode, electrolyte and fuel-electrode. The contacts between electrolyte and electrodes seem to be intact. Figs. 4b and 4c show that the bonding between air electrode and electrolyte was not affected after the 100 cycles. Fig. 4d further shows that the infiltrated SSC-SDC fine particles remain well dispersed in the porous LSGM skeleton after the test. Such an air-electrode structure is deemed beneficial to the retention of battery's performance.[11] The comparison in Fig. 4e and 4f of the interface between fuel-electrode and electrolyte before and after test appears to suggest that

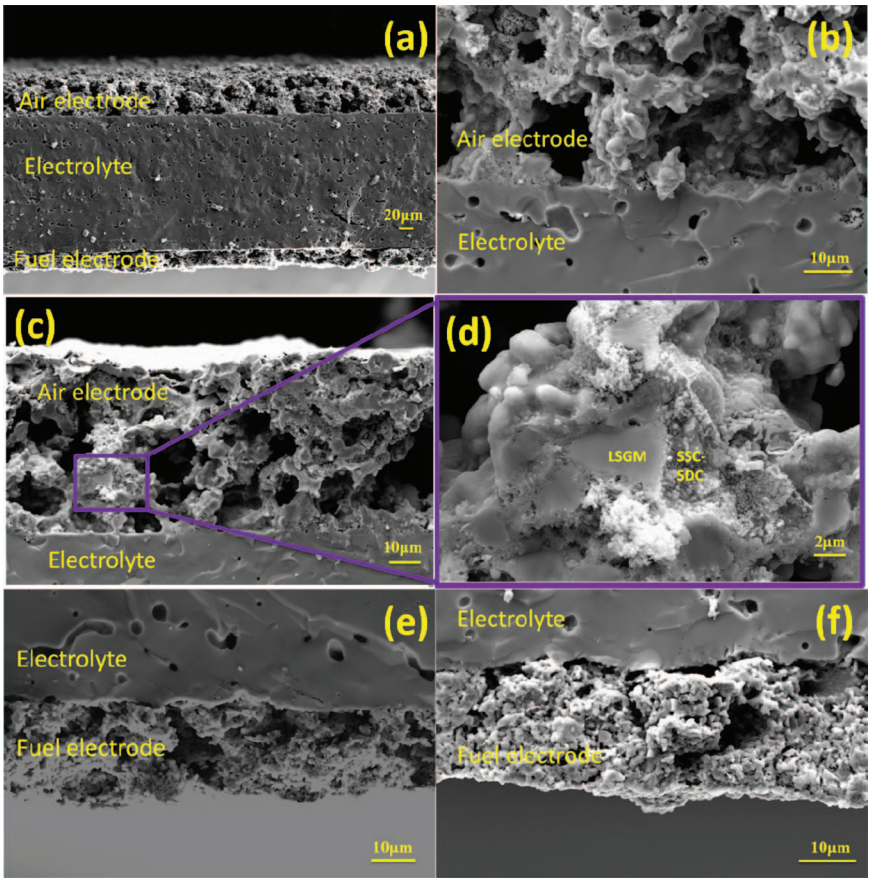

Figure 4. Cross-sectional view of the microstructures of a RSOFC: (a) the whole battery; (b) magnified prior-test air-electrode/electrolyte interface; (c) magnified post-test air-electrode/electrolyte interface; (d) magnified post-test air-electrode with porous LSGM infiltrated by SSC-SDC nanoparticles; (e) magnified prior-test fuel-electrode/electrolyte interface and (f) magnified post-test fuel-electrode/electrolyte interface.

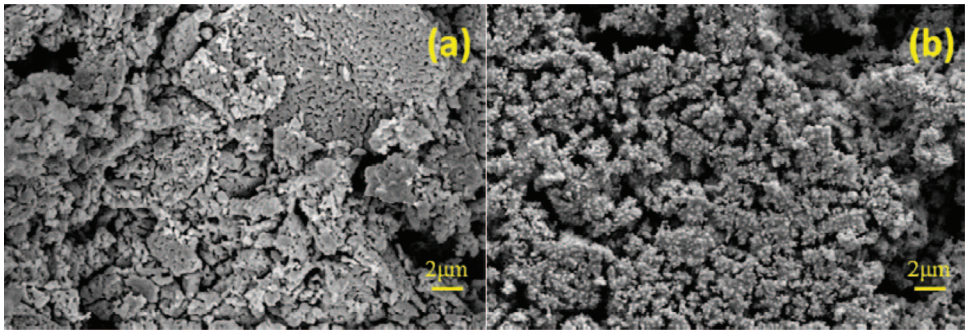

Figure 5. Microstructures of the Fe-FeO energy storage medium; (a) prior test and (b) post test.

the detachment at the interface after the cyclic test could attribute to the increase in the total ASR observed. How to make a good fuel electrode of RSOFC under the testing conditions is, therefore, critical to achieving higher and more stable performance for the battery, according to this study.

It is known that the overall performance of the battery is determined not only by RSOFC, but also by the Fe-based ESM. Our previous study has shown that the Fe-based ESM is capable of retaining its porosity and grain size even after endurance test at 800°C, mainly benefited from the presence of ZrO_2 as the sintering inhibitor.[13] Fig. 5 shows that similar microstructures of the same ESM can also be retained for 650°C. In particular, spherical particles of Fe are visible in Fig. 5b being uniformly distributed across the ESM after the test. No significant changes in the microstructure of ESM can be found to attribute to the degradation of the battery. Therefore, the degradation shown in the durability test should mainly arise from the fuel electrode of the RSOFC.

Conclusion

The recently developed solid oxide Fe-air redox battery has shown potential for use in mid- to large-scale stationary energy storage. To fulfill the requirements of stationary energy storage, cyclic durability of the battery is of great importance. In this study, we demonstrated that the performance of a solid oxide Fe-air redox battery continuously cycled under a current density of 50 mA/cm^2 for 100 times remained rather stable. The battery exhibited an average discharging specific energy of 760 Wh/kg-Fe over the 100 cycles, which is about 77.1% of maximum theoretical specific energy. When compared with the average charging specific energy (= 1,370 Wh/kg-Fe), the battery showed a round-trip efficiency of 55.5%. Post-test examinations suggested that the fuel-electrode in the RSOFC could be a major source of the degradation and performance losses observed in battery's performance, which calls for the development of robust fuel-electrodes for future SOMARBs to achieve a better cyclic stability with higher specific energy and round-trip efficiency.

References

1. Y. C. Lu, H. A. Gasteiger, and Y. Shao-Horn, *J. Am. Chem. Soc.*, **133**, 19048 (2011).
2. Z. Peng, S. A. Freunberger, Y. Chen, and P. G. Bruce, *Science*, **337**, 563 (2012).
3. J. S. Lee, S. Tai Kim, R. Cao, N. S. Choi, M. Liu, K. T. Lee, and J. Cho, *Adv. Ener. Mat.*, **1**, 34 (2011).
4. K. F. Blurton and A. F. Sammells, *J. Power Sources*, **4**, 263 (1979).
5. O. Chusid, Y. Gofer, H. Gizbar, Y. Vestfrid, E. Levi, D. Aurbach, and I. Riech, *Adv. Mater.*, **15**, 627 (2003).
6. F. Cheng and J. Chen, *Chem. Soc. Rev.*, **41**, 2172 (2012).
7. S. A. Freunberger, Y. Chen, N. E. Drewett, L. J. Hardwick, F. Bardé, and P. G. Bruce, *Angew. Chem. Intl. Ed.*, **50**, 8609 (2011).
8. Y. C. Lu, E. J. Crumlin, G. M. Veith, J. R. Harding, E. Mutoro, L. Baggetto, N. J. Dudney, Z. Liu, and Y. Shao-Horn, *Sci. Rep.*, **2**, 715 (2012).
9. L. Öjefors and L. Carlsson, *J. Power Sources*, **2**, 287 (1978).
10. S. R. Narayanan, G. K. S. Prakash, A. Manohar, B. Yang, S. Malkhandi, and A. Kindler, *Solid State Ionics*, **216**, 105 (2012).
11. X. Zhao, Y. Gong, X. Li, N. Xu, and K. Huang, *J. Electrochem. Soc.*, **160**, A1241 (2013).
12. N. Xu, X. Li, X. Zhao, J. B. Goodenough, and K. Huang, *Ener. & Environ. Sci.*, **4**, 4942 (2011).
13. X. Zhao, N. Xu, X. Li, Y. Gong, and K. Huang, *RSC Adv.*, **2**, 10163 (2012).
14. X. Zhao, X. Li, Y. Gong, N. Xu, K. Romito, and K. Huang, *Chem. Commun.*, **49**, 5357 (2013).
15. X. Zhao, N. Xu, Xue Li, Y. Gong, and K. Huang, *ECS. Trans.*, **50**, 115 (2013).
16. X. Zhao, N. Xu, Xue Li, Y. Gong, and K. Huang, *ECS. Trans.*, **45**, 113 (2013).
17. A. Inoishi, S. Uratani, T. Okano, and T. Ishihara, *Phys. Chem. Chem. Phys.*, **14**, 12818 (2012).
18. A. Inoishi, S. Ida, S. Uratani, T. Okano, and T. Ishihara, *RSC Adv.*, **3**, 3024 (2013).
19. A. Inoishi, Y. W. Ju, S. Ida, and T. Ishihara, *J. of Power Sources*, **229**, 12 (2013).
20. A. Inoishi, Y. Okamoto, Y. W. Ju, S. Ida, and T. Ishihara, *RSC Adv.*, **3**, 8820 (2013).
21. K. Huang, R. S. Tichy, and J. B. Goodenough, *J. Am. Ceram. Soc.*, **81**, 2565 (1998).
22. X. Zhao, X. Li, N. Xu, and K. Huang. *Solid State Ionics*, **214**, 56 (2012).
23. Z. Zhan, D. Han, T. Wu, X. Ye, S. Wang, T. Wen, S. Cho, and S. A. Barnett, *RSC Adv.*, **2**, 4075 (2012).